Journal of Thermal Analysis, Vol. 35 (1989) 405-427

CHARACTERIZATION OF HIGH-TECHNOLOGY MATERIALS BY EMANATION THERMAL ANALYSIS

V. Balek

NUCLEAR RESEARCH INSTITUTE, 250 68 ŘEŽ, CZECHOSLOVAKIA

The principles of the emanation thermal analysis, based on the measurement of inert gas release from solids, are given. Results of the computer modelling of inert gas release curves during heating of porous and dispersed samples are demonstrated.

Examples of the characterization of high-tech ceramic materials and raw materials for their preparation by means of emanation thermal analysis are given, such as the evaluation of reactivity and sinterability of ceramics powders, quality testing of intermediate and final products of advanced technology materials (such as thoria, urania, ferrites, superconducting oxide ceramics, etc.).

Introduction

The development of high technology materials with "tailored" properties led to the increased interest to the methods of materials characterization reflecting the structure sensitive properties of materials. One of these methods is the emanation thermal analysis which can be advantageously used for checking and control of the solid state processes taking place during preparation of high technology materials as well as for the quality testing of the raw materials, intermediate and final products of the technologies.

Principle of the emanation thermal analysis[1,2]

The emanation thermal analysis (ETA) is based on the measurement of the inert gas release from samples previously labelled. The high detection sensitivity of radioactive nuclides used for the measurement makes it possible to use very low concentrations of the inert gases (10^{-14} at %) so that no influence of the inert gases on the properties of the solids can be supposed.

The inert gases may be incorporated into the solid samples by several techniques[2], e.g. by the diffusion of the inert gas into the solid at higher pressure and temperature, by ion implantation, or by means of nuclear reaction.

John Wiley & Sons, Limited, Chichester
Akadémiai Kiadó, Budapest

The inert gases can be incorporated into solid samples together with their parent nuclides, e.g. by coprecipitation during the sample preparation or by adsorption on the sample surface. In the latter case the inert gas atoms are incorporated into the surface layers of several tens of nanometers, due to the recoil energy (85 keV/atom) which every ^{220}Rn atom gains in the moment of its formation by the ^{224}Ra decay, according to the scheme

$$^{228}Th \xrightarrow{\alpha} {}^{224}Ra \xrightarrow{\alpha} {}^{220}Rn \xrightarrow{\alpha}$$

The radioactive nuclide ^{228}Th serves as the permanent source (the half life = 1.9 y) of ^{220}Rn (the half life = 55 s).

The inert gas atoms incorporated into solids are situated on the structure defects, such as vacancies, vacancy clusters, grain boundaries etc. The mobility of the inert gases in solids is strongly dependent on the structure and its changes. The structure defects can serve both as traps and as diffusion paths for the inert gas.

When the inert gas atoms are formed by the decay of the parent nuclides within the solids, the diffusion and the recoil mechanism should be taken into account as migration mechanisms of the inert gas in the solid. The recoil plays an especially important role at temperatures where the inert gas diffusion in the solid is negligible, with solids of large surface area.

Computer modelling of the inert gas release from solids

The computer modelling of the inert gas release from solids was used to demonstrate the sensitivity of the emanation thermal analysis to various solid state processes. Theoretical concepts by Kříž and Balek[3,4] and Beckman and Shviryaev[5] and other authors[6] were used for the computer modelling of the inert gas release from dispersed and porous solid samples during heating. Following inert gas release mechanisms were considered:

- inert gas diffusion in pores
- inert gas diffusion in highly defective solid matrix
- release of the inert gas atoms due to the recoil energy.

Following solid state processes were taken into account:

- inert gas diffusion in pores characterized by the effective activation energy of diffusion $E_p \in \langle 160\text{–}280$ kJ/mol$\rangle$
- inert gas diffusion in the highly defective solid characterized by the effective activation energy $E_{sd} \in \langle 240\text{–}300$ kJ/mol$\rangle$
- sintering of porous solid sample characterized by the effective activation energy $E_{ps} \in \langle 160\text{–}280$ kJ/mol$\rangle$.

In Fig.1 we demonstrate the model curves of the temperature dependence of the radon release. Various values of the effective activation energy E_{ps} of sintering and those of the effective activation energy E_{sd} of radon diffusion in the solid matrix were taken into account. With the increase of E_{ps} values the break on the ETA curve shifts to the higher temperatures, as it should be expected. The shape of the temperature dependence of radon release rate in the high temperature range is given by the difference between E_{ps} and E_{sd}. The higher the difference $E_{sd} - E_{ps}$, the more pronounced effect on the ETA curve which indicates the sintering.

In Fig. 2 we demonstrate the results of the computer modelling of radon release rate from the sample during structure changes accompanying phase transitions, chemical transormations, etc., in solids.

For radon diffusion coefficient in initial and resulting phases following expressions can be written:

$$D_1 = D_{1,0}\exp(-E_1/RT) \quad \text{and} \quad D_2 = D_{2,0}\exp(-E_2/RT) \text{ resp.} \qquad (1)$$

The change of the radon diffusion properties during the structure change can be expressed as follows:

$$K = K_o \exp(E_k/RT) \qquad (2)$$

The inert gas behaviour during the sample heating over the whole temperature interval is characterized by the effective diffusion coefficient D_{ef}

$$D_{ef} = (D_1 + K D_2)/(1 + K) \qquad (3)$$

The case demonstrated in Fig. 2 represents common conditions of the radon diffusion in the crystaline solids.

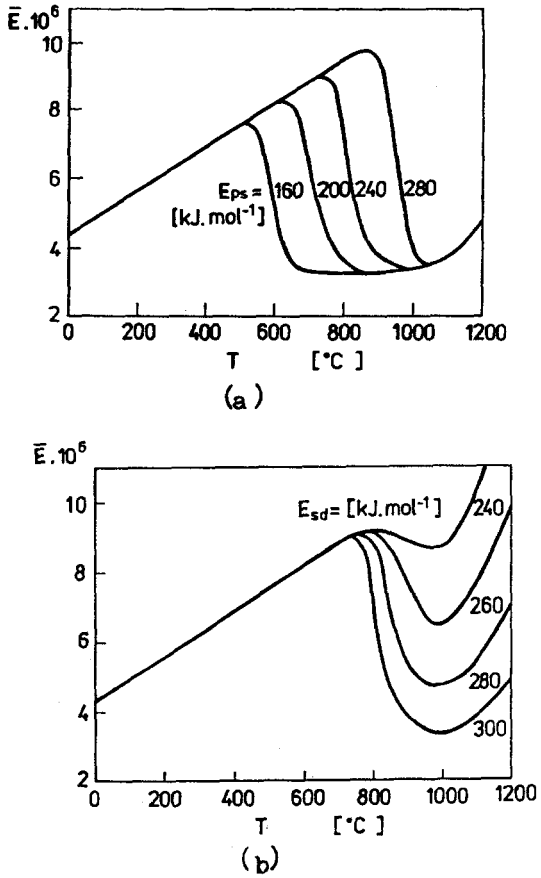

Fig. 1: Results of the computer modelling of

a) the influence of the effective activation energy E_{ps} of the porous sample sintering on the temperature dependence of radon release rate (the E_{sd} value for radon diffusion in the solid equalling 280 kJ/mol)

b) the influence of the effective activation energy E_{sd} of radon diffusion in the solid under constant value of E_{ps} = 200 kJ/mol

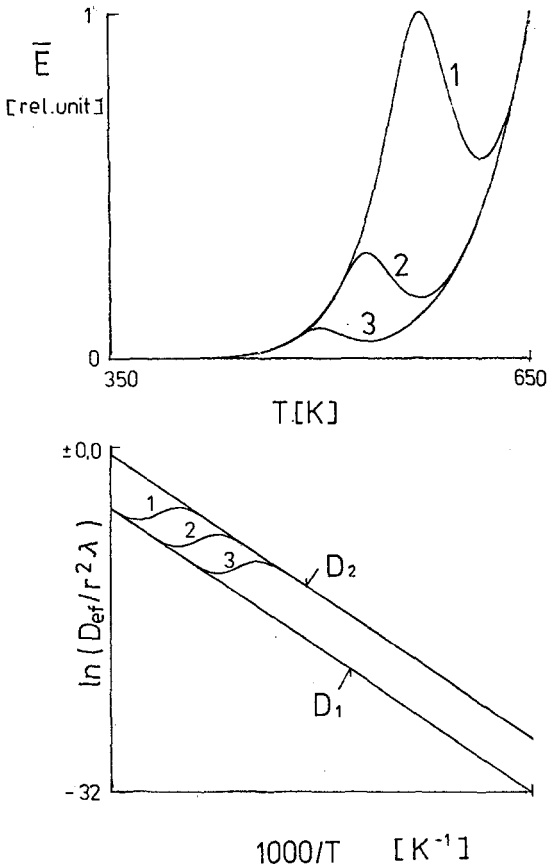

Fig. 2: Results of the computer modelling of the radon release rate during structure changes of solid sample.
The initial and final stage of the structure are characterized by the apparent activation energy values 100 kJ/mol.
The following parameters of the structure change kinetics were considered: E_K = 200 kJ/mol, and $\log K_0$ values - 70, - 75 and - 80 for the curves 1, 2, 3 resp.

Experimental

The solid samples investigated were labelled by ^{228}Th and ^{224}Ra, representing a relative stable source of ^{220}Rn. By this way the labelling of samples enabled us to investigate the behaviours of solids upto the high temperatures in several heating and cooling runs without the necessity to re-label the sample. The parent nuclides of radon were co-precipitated or adsorbed at the sample.

The equipment for emanation thermal analysis permited to measure the trace amount of inert gases, carried from the sample by the carrier gas (air, argon, etc.) into the radioactivity detector. The scheme of the ETA apparatus is given in Fig. 3. The ETA equipment[7] produced by NETZSCH, Selb, FRG gives the possibility of simultaneous measurement of several parameters during thermal treatment of sample (DTA, TG/DTG, detection of gaseous products of reaction, dilatometry etc.).

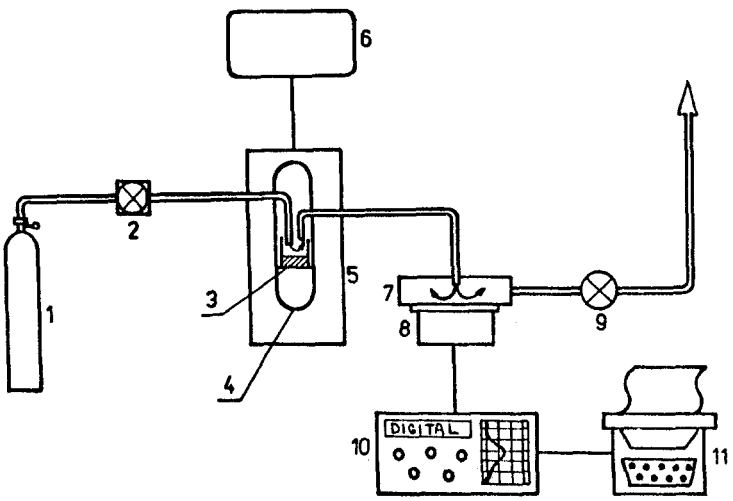

Fig.3 Scheme of the apparatus for emanation thermal analysis
1 - gas supply, 2 - gas flow stabilizer and flow rate meter, 3 - labelled sample, 4 - sample holder, 5- furnace, 6 - temperature controller, 7 - measuring chamber, 8 - radioctivity detector, 9 - flow rate meter, 10 - counts meter, 11 - data processor and printer (plotter).

Examples of the ETA application

1. Preparation of hematite for ferrite production

In Fig. 4a-d the results of ETA, DTA and dilatometry are demonstrated, which were obtained during air heating of various iron salts (Mohr's salt, iron(II) sulphate, iron(II) oxalate and iron (II,III) hydroxocarbonate) at the constant heating rate 10 K/min. The temperature intervals of the salts decomposition were determined from these results, the ETA giving the information on the morphology changes of the intermediate products of thermal decomposition.

The differences in the morphology of the iron (III) oxide samples prepared by heating to 700, 900 and 1100°C were tested by the ETA during the subsequent heating of the samples as the heating rate 10 k/min.

In Fig. 5 the ETA curves are demonstrated which represent the morphology changes of iron (III) oxide differing in the thermal history. The samples were prepared by the decomposition of iron (II,III) hydroxocarbonate and treatment to 700, 900 and 1100°C. By this way the emanation thermal analysis enabled us to characterize the differences in the morphology directly during the heat treatment of the samples, without the necessity to interrupt the treatment.

2. Estimation of the active state (non-equilibrium state) of iron (III) oxide

The influence of the thermal and chemical history on the active state of powdered iron (III) oxide can be assessed from values of the apparent activation energy of radon diffusion determined from the experimental ETA results obtained during heating or cooling of the sample, at temperatures below 0.5 T_m, where T_m is the melting point in the absolute scale. In this temperature range the apparent activation energy of radon diffusion reflects the topochemical defects remaining in the structure of iron (III) oxide after the decomposition of iron salts used for the preparation of the oxide samples. Hüttig[9] and Hedvall[10] called this phenomenon the structure memory of solids.

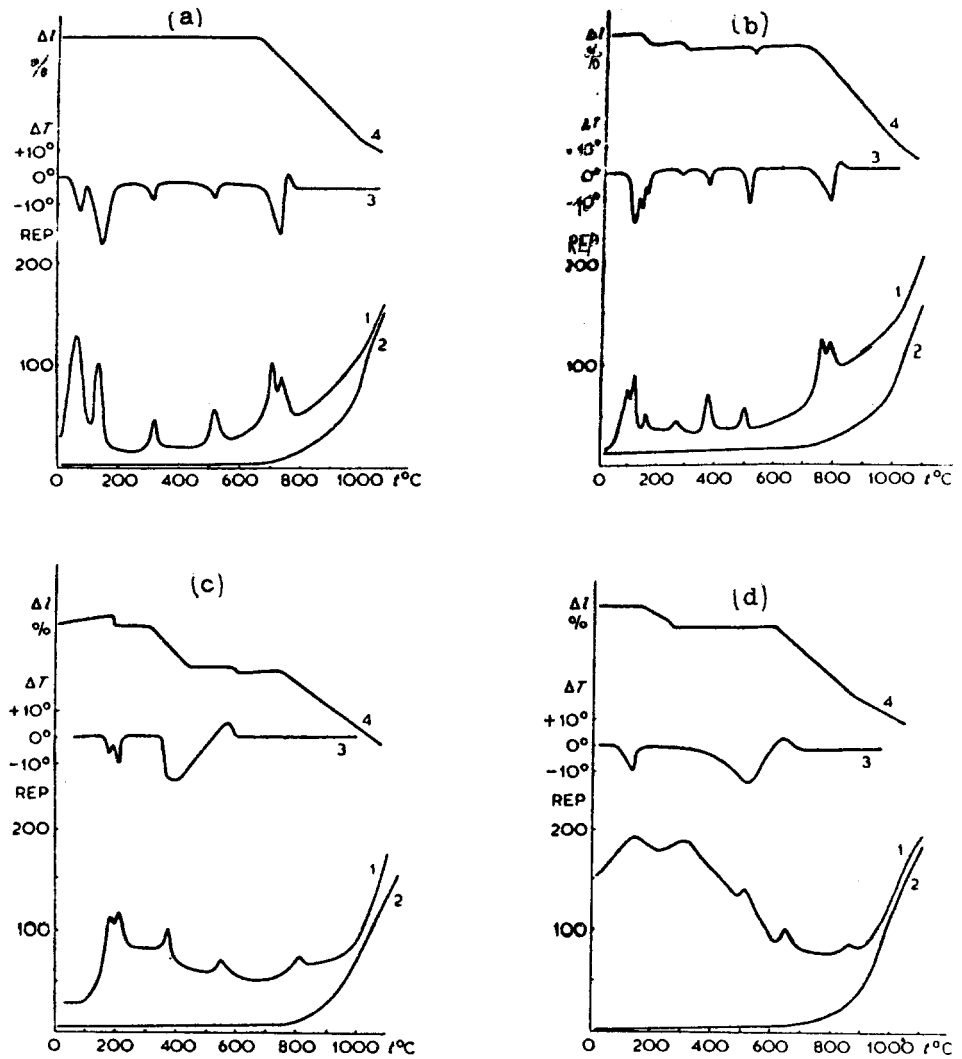

Fig. 4: ETA (curve 1), DTA (curve 3) and dilatometry (curve 4) of various iron (II) salts measured during heating in air at the heating rate 10 K/min; curve 2 is the ETA curve of the sample during second run heating, no changes were observed on the DTA and dilatometry curves during second run heating.

a) iron (II) sulphate heptahydrate
b) Mohr's salt
c) iron (II) oxalate dihydrate
d) iron (II,III) hydroxocarbonate

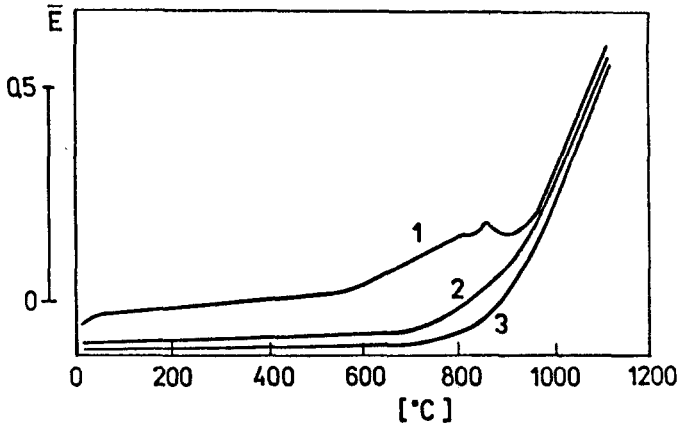

Fig. 5: ETA curves of iron (III) oxide measured during heating in air at the heating rate 10 K/min. The samples were prepared by thermal decomposition of iron (II,III) hydroxocarbonate and heating to 700, (curve 1), 900 (curve 2) and 1100°C (curve 3).

Fig. 6 shows the ETA curves of iron (III) oxide samples prepared by heating various iron salts to 1100°C. The dependence log E_d versus 1/T was used for the evaluation of the values of apparent activation energy of radon diffusion in the samples with various chemical history. The following values of the activation energies were found, corresponding to iron (III) oxide prepared by heating Mohr's salt, iron (II) sulphate, iron (II,III) hydroxocarbonate and iron (II) oxalate: 46, 79, 117 and 126 kcal/mol, resp. The highest values corresponding to iron(III) oxide, from the oxalate, indicated the lowest activity of the solid.

Consequently, the effective activation energy values of radon diffusion in the solids can be used as the parameter for testing the non-equilibrium defects in solids, especially the topochemical defects.

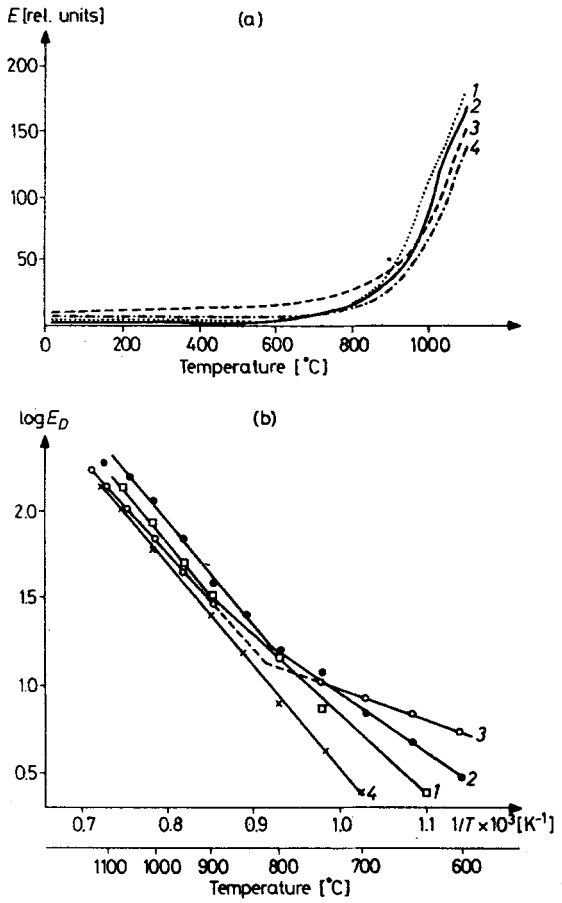

Fig. 6: ETA curves of iron(III) oxide prepared by heating various iron salts to 1100°C in air:
iron(II,III) hydroxocarbonate (curve 1)
iron(II) sulphate heptahydrate (curve 2)
Mohr's salt (curve 3)
iron(II) oxalate dihydrate (curve 4)
a) as dependence of E vs. T
b) as dependence of log E_d vs. 1/T

3. Evaluation of the reactivity of ceramic powders

For evaluation of the reactivity of powders the surface area has been traditionally used. However, the experience showed that in the high temperature reaction, which takes place e.g. in ferrite production, the surface area values do not reflect the real reactivity of powdered iron(III) oxide.

The ETA was used to evaluate the reactivity of iron(III) oxide in the mixture with zinc oxide (1:1 mol) where ZnO component was labelled with ^{228}Th. In Fig. 7 the results of ETA, DTA and dilatometry measurements used for the study of zinc ferrite formation in the mixture $ZnO-Fe_2O_3$ are shown. The surface reaction in the powder mixture in the temperature range 250 - 400°C is indicated by a slight increase of the radon release rate. The highest reaction rate was observed by ETA in the temperature range 650 - 800°C. The break on the ETA curve coresponds to the onset of the structure ordering of zinc ferrite formed. The further increase of E corresponds to the temperature enhanced diffusion of radon in the reaction product. The ETA curve measured during the second heating run was used for evaluation of the radon diffusion characteristics in the zinc ferrite structure, which reflected the defect state of the structure.

In Fig. 8 the ETA curves of 12 reaction mixtures $ZnO-Fe_2O_3$ containing iron(III) oxide with different thermal and chemical histories are summarized. These results were used for evaluating the iron(III) oxide in the mixture with ZnO. The temperatures of the break on the ETA curves served as a parameter for characterization of bulk reactivity of the reaction mixture and are compared with the surface area values of iron(III) samples tested. In the reaction mixture the reference ZnO, labelled homogeneously with ^{228}Th, was used. It was proved by the ETA curves during second run heating that the reaction of zinc ferrite formation was completed during the first heating run (in air, heating rate 10 K/min). Using the second run heating ETA curve (in all cases of the exponential shape) the diffusion characteristics of radon in the zinc ferrite samples prepared were determined.

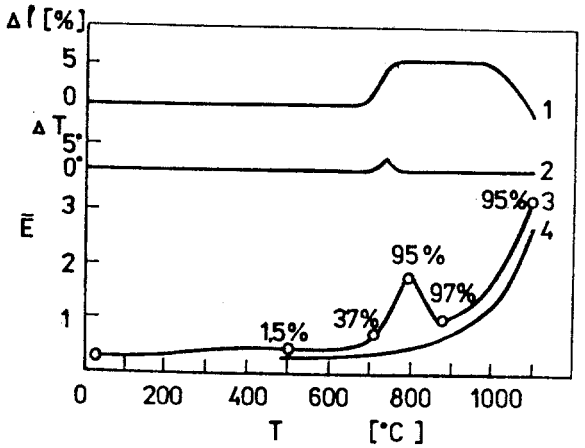

Fig. 7: ETA curve (3), DTA curve (2) and dilatometry curve (1) of 1:1 mol mixture $ZnO-Fe_2O_3$ during heating in air at the heating rate 10 K/min; curve 4 - is the ETA measured during second run heating. No changes on DTA and dilatometry during second run heating were observed. ZnO was labelled with ^{228}Th.

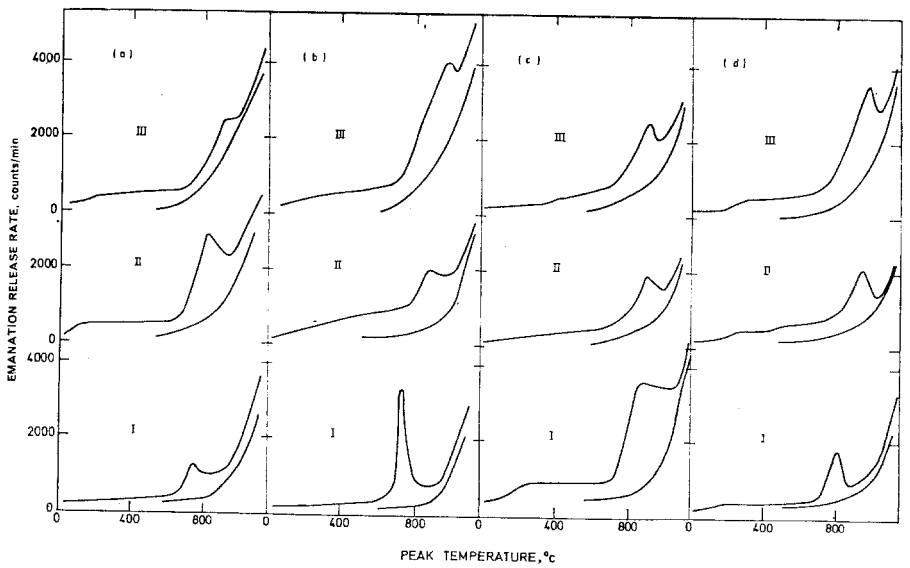

Fig. 8: ETA curves of the 1:1 mol $ZnO-Fe_2O_3$ mixture, ZnO labelled by ^{228}Th. Fe_2O_3 samples were prepared by heating to (I) 700°C, (II) 900°C and (III) 1100°C; a) Mohr's salt, b) iron (II) sulfate, c) iron (II) oxalate and d) iron (II,III) hydroxocarbonate.

Table 1
Reactivities of iron(III) oxide samples with different thermal and chemical histories tested by surface area measurements and by emanation thermal analysis

Initial iron salt	Heating temp., °C	Specific surface (S), m²/g	Peak temp. on the emanogram, °C
Ferrous sulphate heptahydrate	700	9·60	710
	900	0·49	850
	1100	0·16	960
Mohr's salt	700	12·59	740
	900	1·59	810
	1100	0·16	900
Ferrous oxalate dihydrate	700	1·78	860
	900	0·63	900
	1100	0·19	950
Basic carbonate of iron	700	5·89	790
	900	0·87	925
	1100	0·33	980

Table 1 summarizes the reactivities of various iron(III)oxide samples towards ZnO as obtained by ETA measurements, and the surface area values obtained by adsorption measurements. Some discrepancies were observed in the reactivity testing of the samples by means of the two methods.

However, no correlation was found between the reactivity estimations by means of ETA and surface area of commercial iron (III) oxide samples. For example, with the sample denoted "for ferrites" surface area 3.9 m^2/g the ETA break was observed at 720°C, whereas with the sample "p.a.", surface area 14.8 m^2/g, the lower activity was found: ETA break at the temperature 820°C.

When zinc oxide was air heated to 800 and 1200°C resp., the surface area decreased from 0.9 to 0.1 m^2/g, whereas the reactivity of the ZnO samples in the mixture with iron(III) oxide increased. The enhanced reactivity of zinc oxide was supposed[11] to be caused by the non-stoichiometry of the sample ZnO_{1-x}.

The emanation thermal analysis was recommended as the method suitable for the reactivity estimation of the feed materials for ferrite production.

4. Testing of the sinterability of powders

The ETA enabled us to follow the changes of the surface area and morphology caused by the sintering of powders. The kinetics

of the sintering process both in isothermal and non-isothermal conditions were studied in thoria, iron(III) oxide[12], urania[13] and other oxide materials[14]. In Fig. 9 the ETA curves of thoria powder (surface area 18 m^2/g) are demonstrated, obtained during air heating at the heating rate 10 K/min. As it follows from Fig. 9a, in the temperature range 700 - 850°C, the smoothening of the surface takes place, which was proved by the microphotographs. The kinetics of this early stage of sintering investigated by means of ETA in isothermal conditions at temperatures 705, 735, 780 and 825°C is demonstrated in Fig. 9b. It can be supposed that the early sintering stage (smoothening of the surface) of thoria powder is controlled by one mechanism. The formal expression was suggested for the kinetics of the morphology changes of the thoria surface, as given in Eq. 4

$$\Delta \vec{E} \sim S = \text{const.} \; \text{time}^n \qquad (4)$$

where n = 0.64.

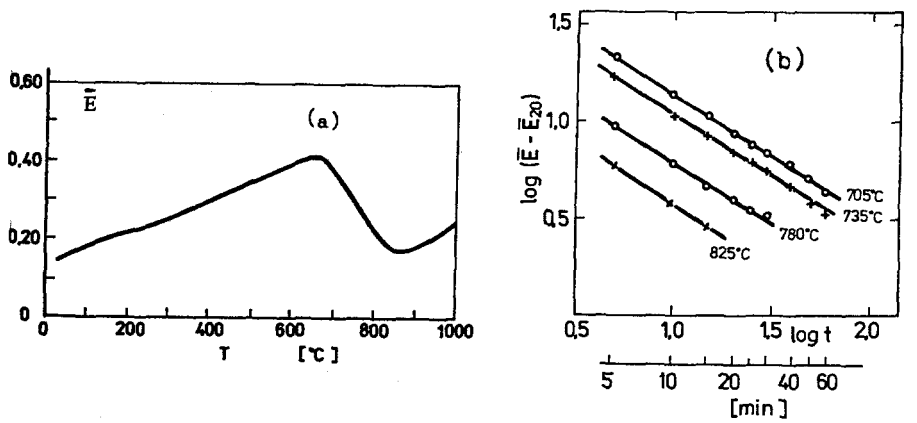

Fig. 9: The ETA curves of thoria powder (surface area 18 m^2/g)
a) measured during air heating at the heating rate 10 K/min
b) measured during isothermal treatment in the temperature range 705 - 825°C.

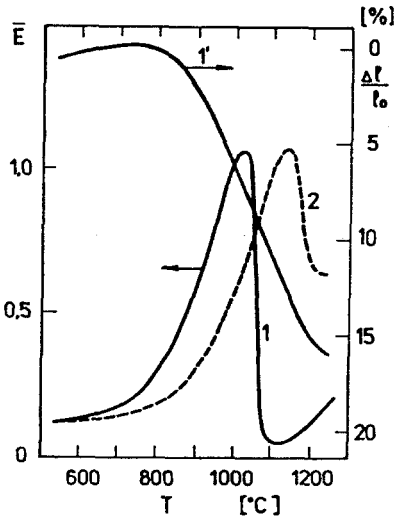

Fig. 10

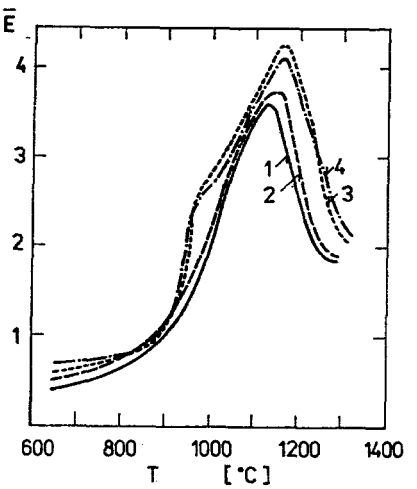

Fig. 11

Fig. 10: ETA curves (1,2) and dilatometry curve (1') of iron(III) oxide -(BAYER 1360 WF, surface area 2.8 m^2/g)measured during air heating at the heating rate 5 K/min. Curves 1 and 1' correspond to pellets, curve 2 corresponds to powder of iron(III) oxide.

Fig. 11: ETA curves of iron(III) oxide powder -(BAYER 1360 Bayferrox, surface area 2.7 m^2/g)measured during air heating at various heating rates 2.5; 5; 10 and 16 K/min.

In Fig. 10 the ETA curves of iron(III) powder and pellet are compared indicating the effect of the pressure of 375 MPa/cm^2 on thermal behaviour of powdered sample. The comparison of the ETA curve of the pellets and the dilatometry curve of the same sample are in an excellent agreement. The advantage of the ETA application for investigating the free sintering consists in the possibility to study the ceramics powders.

The results of the non-isothermal kinetic study of the sintering of iron(III) oxide are demonstrated in Fig. 11. The effective energy of sintering E_{ps} = 214 kJ/mol was determined from the shift of the ETA break in Fig. 11, the value being in a good agreement with the results of other authors[15].

5, Diagnostics of intermediate products of oxide materials

The ETA application is especially advantageous in cases of investigation of geleous and poorly crystallized materials where traditional methods of materials' diagnostics, such as X-ray difraction, do not give satisfactory results.

The voluminous precipitates and geleous inorganic materials are characterized by the high permeability of inert gas (radon). In Fig. 12 the changes of the radon release rate (ETA curve) and the dilatometry measurement results are compared for urania xerogel droplets, prepared by sol-gel technique. In the temperature range 750 - 950°C the decrease of the emanation rate indicates the recrystallization of urania xerogel, whereas no change on the dilatometry curve was observed. By further heating above 1000°C, when the shrinkage of the sample takes place, the radon release is at first enhanced (due to the radon diffusion release) and further it drops (when the densified structure hinders the radon release[13]

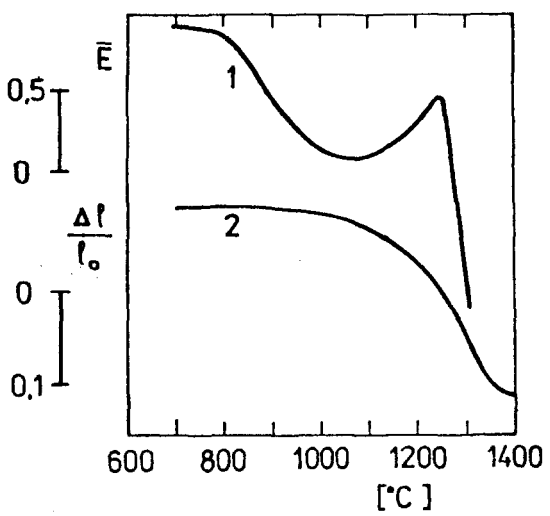

Fig. 12: The ETA curve (1) and dilatometry curve (2) of urania xerogel droplet measured during heating in argon+5%H_2 at the heating rate 5 K/min.

Various urania xerogel prepared under different conditions (gelation additive concentration, washing, drying, aging,etc.) were characterized by means of ETA. The radon diffusion probe indicates sensitively the changes of the morphology of xerogel samples, which gives the possibility to reveal even very fine changes of materials caused by variation of technological conditions in the preaparation of urania.

Fig. 13 demonstrates the differences in thermal behaviours of fresh geleous sample (curve 1) and of water aged xerogel (curve 2). The ETA was used in the study of thermal behaviour of other geleous materials, such as silicagel etc.

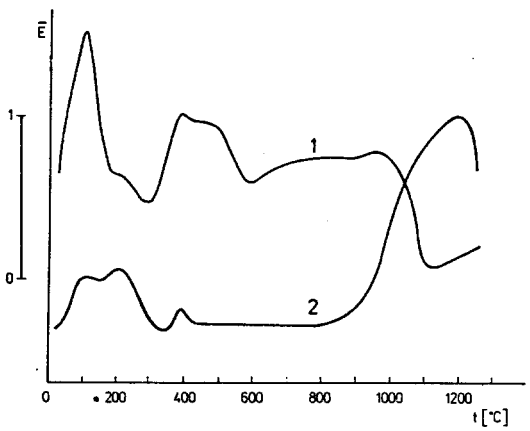

Fig. 13: ETA curves of urania geleous samples obtained during thermal treatment in argon+5% H_2 at the constant heating rate 5 K/min. Curve 1 corresponds to the freshly prepared gel, curve 2 corresponds to the urania gel aged during 30 days in wet conditions.

The ETA was applied for characterization of intermediate products of rutile prepared by calcination of ilmenite hydrolysate. The minor impurities present in the feed hydrolysate have to be washed out or suppressed by the suitable admixtures aiming to produce a pigment of high quality. The ETA curves in Fig. 14 represent the characterization of three samples of ilmenite hydrolysate treated in different ways (washing aiming to remove the residual sulphate ions and adding various cations). It is obvious that the diminishing sulphate anions content leads to

the decrease of the anatas recrystallization temperature from 600 to 400°C, the admixture of 0.5 % ZnO leads to the enhanced formation of rutil at temperatures above 900°C[14].

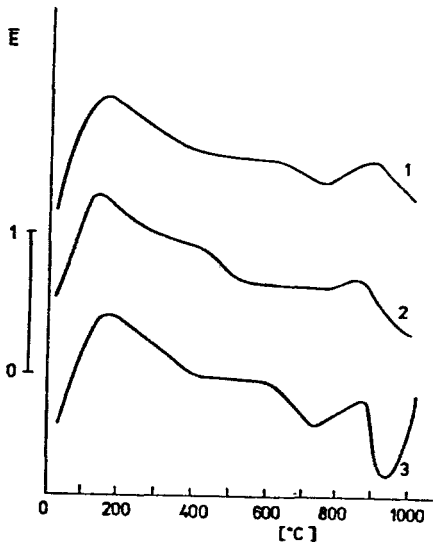

Fig. 14: The ETA curves of the ilmenite hydrolysis product used as feed material for rutil production.
The ETA curves were measured during heating in air at the heating rate 10K/min.
curve 1 - hydrolysis product as prepared, containing 0.3% sulphate ions
curve 2 - sample where residual sulphate ions were removed by ammonia digestion
curve 3 - sample 1 containing 0.5% ZnO

6. Diagnostics of oxide ceramics - high temperature superconductors

Most recently the emanation thermal analysis was used for checking the preparation of Y $Ba_2Cu_3O_{7-x}$ superconducting ceramics. Fig. 15 shows the ETA, TG and DTA results obtained during heating of Y,Ba,Cu oxalate coprecipitate in oxygen.

The ETA results (curve 1, Fig. 15) of the feed oxalate mixture reflect in the temperature range 300 - 750°C the stepwise microstructure changes accompanying the formation of the intermediate and final oxide products. In this temperature range the TG and DTA do not give any effect. The decrease of radon release rate above 750°C indicates apparently the formation of the perovskite phase, whereas the decrease of E above 850°C was ascribed to the sintering of the powdered sample[16].

In Fig. 16 the ETA curve demonstrates the migration of radon in the superconducting oxide material $YBa_2Cu_3O_{7-x}$. At the same time in Fig. 16 the changes of oxygen stoichiometry X of the

material of this composition are demonstrated[17,18]. As it follows from the comparison of the curves 1 and 2, Fig. 16 in the course of the oxygen in-take by the sample in the temperature range 220 - 440°C the increase of the radon release rate E was observed. This may be explained by the fact that the oxygen vacancies are maintained ordered in this temperature range, which makes easier the radon release from the sample.

In the temperature interval 380 - 550°C the decrease of the radon release rate was observed, indicating that the oxygen vacancies randomization is connected with the distortion of the pathes of radon atoms to escape and/or by trapping of radon atoms by the defect sites formed in this temperature interval. Supposing that the interatomic space in c-axis of the perovskite structure of this material is approx. 0.39 nm, the radon atoms of the size 0.19 nm serve as the probe of the changes of the microstructure.

As indicated by X-ray patterns, the orthorombic structure of the perovskite phase changes into tetragonal structure at approx. 600°C[18]. At this temperature the radon release rate starts to increase indicating the microstructure changes in the solid sample.

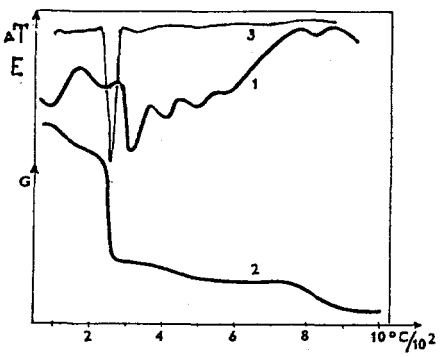

Fig. 15: ETA curve (1), TG curve (2) and DTA curve (3) of the Y, Ba, Cu oxalate coprecipitate during heating in oxygen at the heating rate 5 K/min. The parameters E, G, and Δ T are given in arbitrary units.

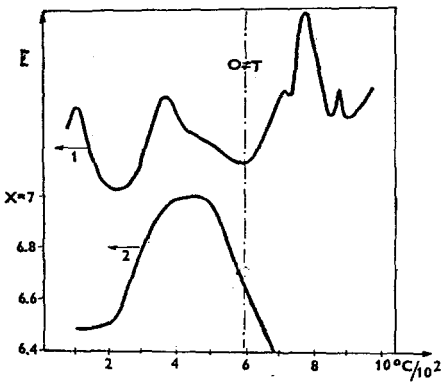

Fig. 16: ETA curve of the $YBa_2Cu_3O_{6.5}$ measured during heating in oxygen, heating rate 5 K/min (curve 1) compared with the results of oxygen stoichiometry changes[17] (curve 2).

Similarly, the ETA was used for diagnostics of thermal behaviour of the superconducting material containing Bi-Ca-Sr-Cu-O in the ratio 4:3:3:4. This material has two superconducting transitions, namely at 80-85 K and at 110 - 114 K. The sample prepared by a long time heat treatment to the temperature not exceeding 850°C has only the transition at 80 - 85 K, however, after the short heating of the material to 880°C the second transition at 110-114 K appeared.

The aim of the ETA application to the diagnostics of this system was to study the process taking place during these thermal treatment. As it follows from Fig. 17, in the sample heated to 850°C in air the enhanced radon mobility was observed above 650°C both during sample cooling and reheating. The markedly pronounced drop of the radon release rate at temperatures above 880°C can be ascribed to the melting of one of the component in the sample.

Especially perspective application of the emanation thermal analysis in the diagnostics of the special ceramic materials with "tailored" properties may enable to reveal the fine changes in the microstructure of the ceramic materials which are responsible for maintaining or degradation of the requested properties.

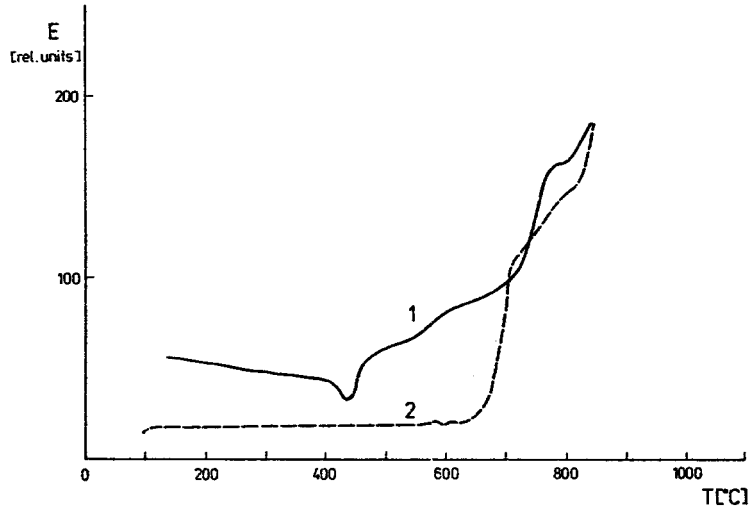

Fig. 17a

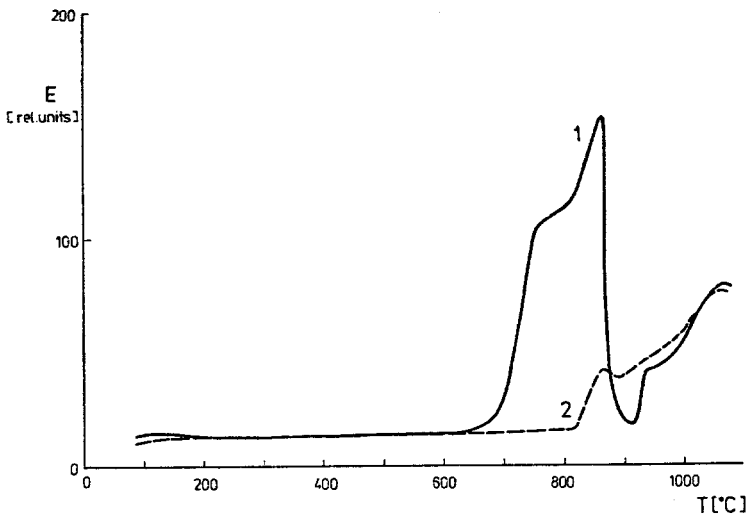

Fig. 17b

Fig. 17: ETA curves of the superconducting material of the composition Bi-Ca-Sr-Cu-O in the ratio 4:3:3:4
a) obtained during first run of air heating (curve 1) and cooling (curve 2) to 830°C at the rate of 5 K/min
b) obtained during second run of air heating (curve 1) and cooling (curve 2) to 1100°C at the rate of 5 K/min

7. Further applications of emanation thermal analysis

It should be mentioned here that the emanation thermal analysis found advantageous application not only in the characterization of ceramic materials but also in evaluating reactivity of hydraulic binders towards water and water vapour, namely the influence of various temperatures and presenceof admixtures on the hydration of clinker minerals[19]. The advantage of the ETA application consists in the investigation of microstructure changes taking place during hydration in situ , without the necessity to interrupt the hydration process.

The ETA found the application also in the field of the characterization of coals, during the heating and cooling. Further fields of the ETA application will be found; especially perspective are the environmental technology, building materials etc.

Conclusion

The emanation thermal analysis has been demonstrated as a suitable tool for evaluation of the structure defect changes, for testing the sinterability and reactivity of ceramic powders, as well as for quality checking intermediate and final products in the advanced technology materials.

References

1. V. Balek, Thermochim.Acta 22 (1978) 1
2. V. Balek, J. Tölgyessy, Emanation Thermal Analysis and other radiometric emanation methods, in Comprehensive analytical chemistry (Ed. G. Svehla), Vol. XII.C, Elsevier Publ.Co. 1984, 209 pp.
3. J. Kříž, V. Balek, Thermochim.Acta 78 (1984) 377
4. J. Kříž, V. Balek, Thermochim. Acta 110 (1987) 245
5. I.N. Beckman, A.A. Shviryaev, Radiokhimia, 29 (1987) 384
6. R. Kelly, Hj. Matzke, J. Nucl. Mat. 20 (1976) 171
7. W.D. Emmerich, V. Balek, High Temp. - High Presss. 5 (1973)67
8. V. Balek, J. Mat. Sci. 5 (1971) 166
9. G.F. Hüttig, Z. Elektrochem. angew. phys.Chem.47 (1941) 282
10. J.A. Hedval, Solid State Chemistry, Elsevier 1969
11. V. Balek, J. Amer. Cer. Soc. 53 (1970) 540
12. V. Balek, Sprechsaal-Ing. glass and ceram.Mag. 116 (1983)978
13. V. Balek, M. Vobořil, V. Baran, Nucl. Tech. 50 (1980) 53
14. V. Balek, Sprechsaal-Int. glass and ceram.Mag. 118 (1985)606

15. R. L. Coble, J. Amer. Cer. Soc. 41 (1958) 55
16. V. Balek, J. Šesták, Thermochim. Acta 133 (1988) 23
17. P. Strobel et al. Letters to Nature 327 (1987) 306
18. T. Ozawa et al., Thermochim. Acta 124 (1988) 147
19. V. Balek, Thermochim. Acta 72 (1984) 147

Zusammenfassung - Es werden Grundlagen für die Emanationsthermoanalyse /ETA/ auf der Basis der Messung der Inertgasfreisetzung bei Feststoffen gegeben. Ergebnisse von computermodellierten Inertgasfreisetzungskurven bei Erhitzen von porösen und dispersen Proben werden angeführt.

Weiterhin werden Beispiele für die mittels ETA durchgeführte Charakterisierung von Spitzentechnologiekeramikmaterialien und den Rohstoffen zu deren Herstellung gegeben: Auswertung von Reaktivität und Sinterbarkeit von Keramikpulver, Qualitätskontrolle der Zwischen- und Endprodukte aus modernen Rohstoffen /wie z.B. Thorerde, Uranerde, Ferrit, supraleitende Oxidkeramiken usw./.

Резюме - Представлены принципы эманационного термического анализа, основанного на измерении инертного газа, выделяющегося из твердых тел. Представлены результаты компьютерного моделирования кривых выделения инертного газа при нагревании пористых и дисперсных образцов. С помощью эманационного термического анализа проведена характеристика высоко-технологичных керамических материалов и исходного для них сырья, заключающаяся в определении реакционной способности и спекаемости керамических порошков, качественной проверке промежуточных и конечных продуктов получаемых высоко-технологичных материалов / ферритов, окиси тория, окиси урана, сверхпроводящей оксидной керамики и др. /.